ACS OMEGA

http://pubs.acs.org/journal/acsodf

Article

Synthesis and Study of a New Type of Nonanionic Demulsifier for Chemical Flooding Emulsion Demulsification

Lixin Wei, Lin Zhang,* Meng Chao, Xinlei Jia,* Chao Liu, and Lijun Shi

Cite This: *ACS Omega* 2021, 6, 17709−17719

Read Online

ACCESS | Metrics & More | Article Recommendations

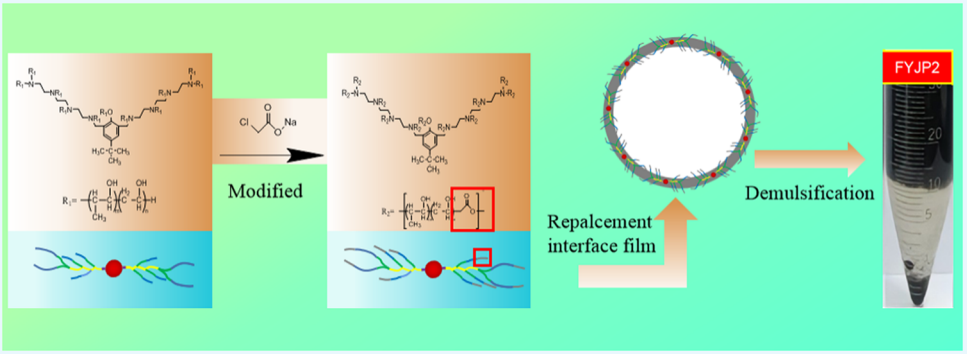

ABSTRACT: The application of chemical flooding improves the stability of the produced emulsion, which reduces the demulsification efficiency of conventional demulsifiers. To improve the demulsification effect, in this paper, a new multibranched nonanionic polyether demulsifier, FYJP, was prepared by grafting carboxylate based on a nonionic demulsifier. The FYJP demulsifier could generate an initiator through *p*-*tert*-butylphenol, triethylenetetramine, and methanol, which was polymerized with ethylene oxide (EO) and propylene oxide (PO) to produce a nonionic polyether demulsifier. Sodium chloroacetate was used to modify the polyether demulsifier to obtain a new type of nonanionic polyether demulsifier. The FYJP polyether demulsifier was characterized by the hydrophilic−lipophilic balance (HLB) value, relative solubility (RSN), and surface activity of the demulsifier, and the demulsification mechanism was analyzed by a microscopic demulsification process test, and the effect of demulsifier dosage on the demulsification effect was discussed. Meanwhile, a dehydration test was carried out. The experimental results showed that the highest dehydration rate of the demulsifier was 94.7% at 85 °C, 100 ppm demulsifier dosage, 50 mL of a W/O emulsion, and 120 min demulsification time. The abovementioned studies show that FYJP is an effective demulsifier for chemical flooding emulsions, and this work promises to provide a reference for future demulsifier research.

INTRODUCTION

To improve oil recovery, chemical flooding has gradually replaced conventional primary and secondary oil recovery techniques such as water flooding and gas flooding.[1−3] The use of chemical flooding to enhance oil recovery has been proven to be effective, and the injection of chemicals such as surfactants makes the production of emulsions easier.[4−6] The formation of an emulsion is due to the interaction of solid impurities, colloids, asphaltene, and other components in crude oil as well as chemical reagents in the process of crude oil production and operation, which forms a rigid, viscoelastic, and stable interface membrane at the oil−water interface.[7−12] This interfacial membrane makes the emulsion very stable.[13,14] The presence of emulsions is hazardous to crude oil production systems, since water may lead to equipment corrosion, pump malfunction, and even safety problems.[15,16] Mechanical, electrical, thermal, and chemical demulsifications are the common demulsification and dehydration techniques for crude oil. Among them, the chemical demulsification method has been widely studied because of its rapid and efficient demulsification.[17−21] Alves et al. analyzed the demulsification activity of a demulsifier based on a synthetic chemical surfactant of castor oil and discussed the demulsification mechanism. The maximum water separation of the demulsifier was about 90% in a bottled experiment.[22] Chen et al. used propylene trimethoxy silane to wrap Fe_3O_4 in a hyperbranched polyamide and condensation to synthesize a new magnetic-response demulsifier. By characterization and demulsification experiment analysis, the new demulsifier was

Received: May 5, 2021
Accepted: June 22, 2021
Published: July 2, 2021

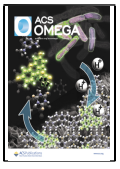

https://doi.org/10.1021/acsomega.1c02352
ACS Omega 2021, 6, 17709−17719

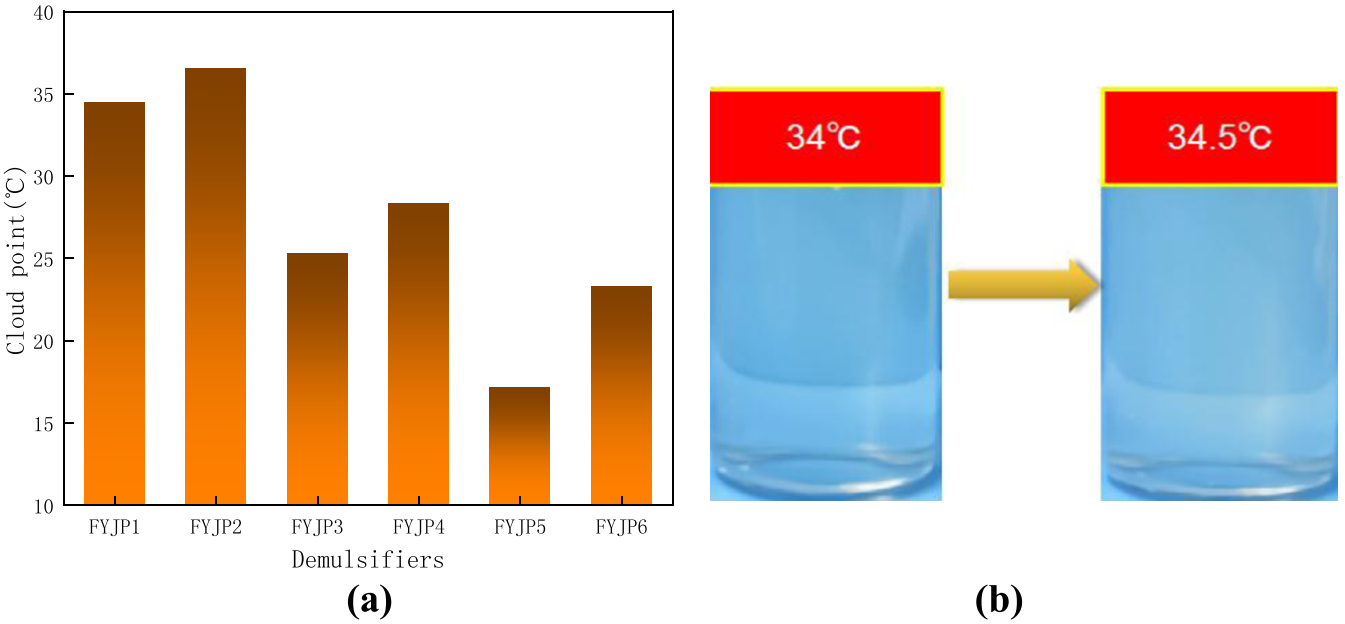

Figure 1. (a) Cloud point of the FYJP series demulsifiers and (b) changes in the FYJP1 aqueous solution at the cloud point.

shown to have good demulsification performance, and the demulsification efficiency reached 97%.[23] Most chemical demulsifiers are amphiphilic nonionic surfactants, consisting of hydrophilic and hydrophobic parts (such as poly(ethylene oxide) (PEO) and poly(propylene oxide) (PPO) blocks of block polyether demulsifiers). A chemical demulsifier can reduce the tension of an oil−water interface film, has higher surface activity, is easy to adsorb on the oil−water interface, and can replace the old, more stable interface film with an easily breakable interface film to achieve the goal of demulsification and dehydration.[24−29] However, at the moment, the stability of emulsions is getting higher and generally nonionic demulsifiers fail to better meet the demulsification requirements.[30] Therefore, it is necessary to refine the chemical demulsifiers. The demulsifying effect of a demulsifier can be improved by physical (compound) or chemical (cross-linking and chain extension) treatments.[31−33]

p-tert-Butylphenol (PTBP) is a common chemical substance, mainly used in the synthesis of *p-tert*-butylphenolic resin, which is widely used in various fields.[34] Because of its low price and good demulsification effect, it is usually used as one of the main materials for preparing a polyether demulsifier as a starting agent. In this paper, a new type of nonanionic demulsifier was prepared on the basis of nonionic demulsifier, the carboxylic acid was grafted into the water soluble and oil soluble blocks of nonionic demulsifier by chain extension chemical teratment, while increasing the molecular weight of the demulsifier and nonionic retaining the properties of nonionic part, it can hydrolyze the anion in solution. At the same time, the demulsifier adsorbed on the oil−water interface replaces part of the active substances, reduces the strength of the interface film, further reduces the stability of the emulsion, and increases the demulsification effect.[35] In this paper, a new type of nonanionic block polyether demulsifier was prepared by using a *para*-tertiary butylphenol (PTBP) initiator; then, propylene oxide (PO) and ethylene oxide (EO) are used for the synthesis of a series of nonionic polyether demulsifiers, and finally, sodium chloroacetate is added to realize successful synthesis of modified nonanionic block polyether demulsifiers. The demulsifier was characterized by the hydrophilic−lipophilic balance (HLB) value, relative solubility (RSN), and surface activity, and the optimal demulsifier dosage was determined. Finally, a dehydration test was used to determine the optimal nonanionic block polyether demulsifier. This strategy can effectively improve the dehydration efficiency of demulsifiers and provide a reference for demulsification and dehydration of emulsions.

RESULTS AND DISCUSSION

Hydrophilic and Lipophilic Balance HLB, Cloud Point, and RSN Values. The abovementioned tests measured the cloud points of all demulsifiers. Figure 1a shows the cloud points of all demulsifiers in the FYJP series. Figure 1b shows the image of the FYJP1 polyether solution when it reaches the cloud point, and the change of the solution from transparent to turbid can be clearly observed. For synthetic polyether demulsifiers with different proportions, the dehydration of hydrophilic groups holds the key to cause the cloud point. A longer hydrophilic group chain can enhance hydration and improve the solubility of the demulsifier, and the cloud point also increases.[36] On the contrary, the increase of hydrophobic groups will lead to a decrease in the turbidity point. It can be seen from the figure that under certain PO conditions, the cloud point increases with the increase in the EO content. When the EO content is constant, the cloud point decreases with the increase in the PO content.[37,38]

The HLB value can be calculated by the formula using the measured cloud points.[7] The HLB value shows the degree of hydrophilicity or oleophilicity of a polyether demulsifier. The larger the HLB value, the stronger the hydrophilicity, and the smaller the HLB value, the stronger the lipophilicity.[44] The relative solubility RSN value is similar to the HLB value, which is also used to evaluate the hydrophilic and oleophilic properties of demulsifiers.[39] At present, it is considered that a demulsifier is lipophilic when the RSN value is less than 13 and hydrophilic when the RSN value is greater than 17. When the RSN value is in the range of 13−17, the demulsifier has both lipophilic and hydrophilic properties.[40−42] The calculated

https://doi.org/10.1021/acsomega.1c02352
ACS Omega 2021, 6, 17709−17719

HLB values and measured RSN values are shown in Table 1. As can be seen from the table, when the PO content is constant, both HLB and RSN values increase with the increase in the EO content. When the EO content is constant, the HLB and RSN values decrease with the increase in the PO content.

Table 1. Cloud Point, HLB Values, and RSN Values of FYPJ Series Samples

demulsifiers	cloud point (°C)	HLB	RSN
FYJP1	34.5	7.4	15.7
FYJP2	36.4	7.6	16.1
FYJP3	25.3	6.5	13.6
FYJP4	28.6	6.8	14.3
FYJP5	17.3	5.7	11.2
FYJP6	23.2	6.3	11.7

Determination of Surface Tension. Figure 2a shows the change curve of surface tension of a demulsifier at different concentrations in an aqueous solution at a test temperature of 80 °C. Surface tension is one of the important properties to evaluate demulsifiers.[43,44] Compared with the blank control experiment, it can be found that the FYJP series polyether demulsifiers can significantly reduce the surface tension of the aqueous solution. It can also be seen that their ability to reduce the surface tension is roughly the same; all of them can reduce the surface tension of the aqueous solution to about 32 mN·m^{-1}. This indicates that the surface activity of the FYJP polyether demulsifier is higher than the surface activity of a natural emulsifier in the emulsion, which can make the interfacial tension lower, so that the FYJP polyether demulsifier can preferentially adsorb on the oil−water interface and replace the original natural active film, and the interface film formed is more prone to rupture so as to achieve the demulsification effect. It can be observed that at a low concentration of the demulsifier, the surface tension of the aqueous solution decreases rapidly with an increase in the concentration. When the concentration reaches a certain level, the decrease in surface tension becomes slow. With a further increase in the concentration, the surface tension basically reaches equilibrium. The surface tension curve usually presents double inflection points.[45] The range between the double inflection points is the cmc range of a polyether. The second inflection point is generally considered to be the value of the polyether cmc.[46,47] Wider molecular weight distribution of block polyethers, the change of the conformation of molecular segments at the gas−liquid interface, and the formation of monomolecular micelles in an aqueous solution before the critical micelle concentration of polyethers can all lead to the formation of double inflection points.[48,49] Comparing the different FYJP polyether demulsifiers, it can be found that the cmc value increases with the increase in the EO content when the PO content is constant. When the EO content is constant, the cmc value decreases with the increase in the PO content. This is because when EO increases, the hydrophilicity of polyether increases and the cmc value increases accordingly. When the PO content increases, the hydrophobicity of polyether increases, making micelle formation easier and resulting in the decrease in cmc.[50,51]

Figure 2b shows that the surface tension of the FYJP1 aqueous solution changes with the concentration of polyether at 40, 60, and 80 °C. The surface tension gradually decreases with an increase in solution temperature and the cmc significantly decreases, indicating that temperature can improve the adsorption capacity of the FYJP polyether demulsifier, thus promoting the micellization of the solution. The first inflection point decreases with increasing temperature, indicating that the surface activity of the demulsifier increases with increasing temperature, thus promoting the ability to reduce surface tension.

Influence of Demulsifier Dosage on Demulsification Performance. The demulsification and dehydration experiments of an FYJP polyether demulsifier with dosages of 20, 50, 100, 150, and 200 ppm were carried out for 120 min at 85 °C. The experimental data graph is shown in Figure 3. As can be seen from the figure, with the increase in dosage, the dehydration rate of the FYJP series demulsifiers gradually increases. Among them, the demulsification rates of FYJP2 and

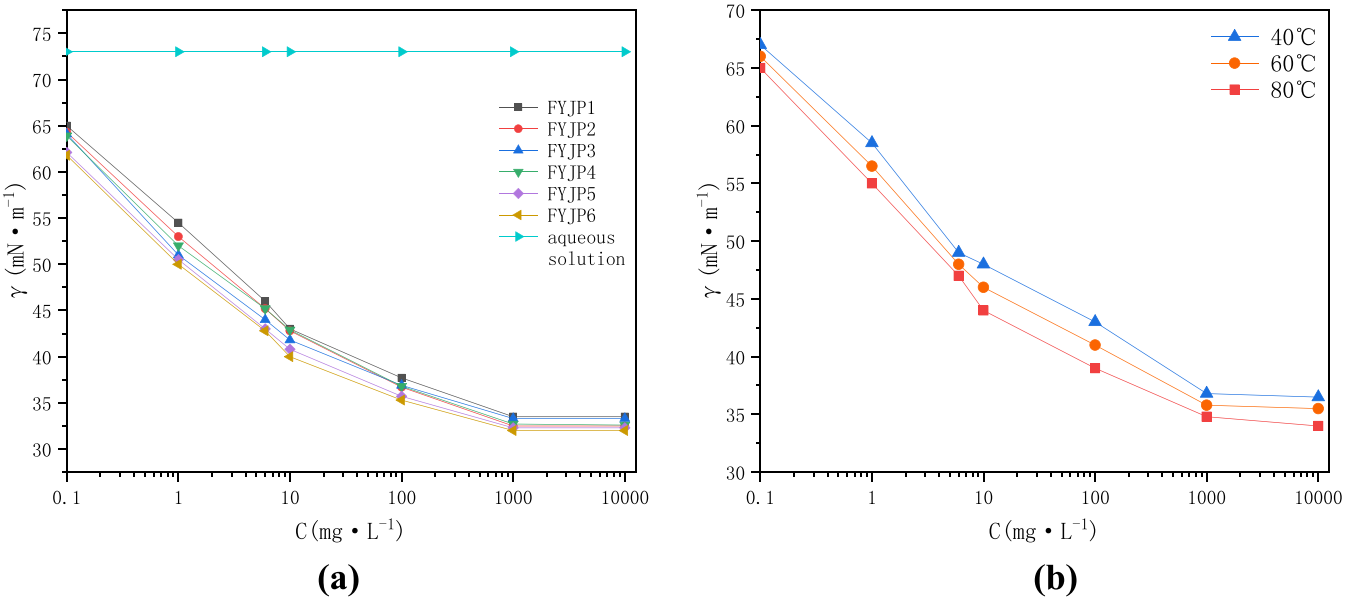

Figure 2. (a) FYPJ series surface tension curves at 80 °C and (b) surface tension of FYJP1 under different temperature conditions.

https://doi.org/10.1021/acsomega.1c02352
ACS Omega 2021, 6, 17709−17719

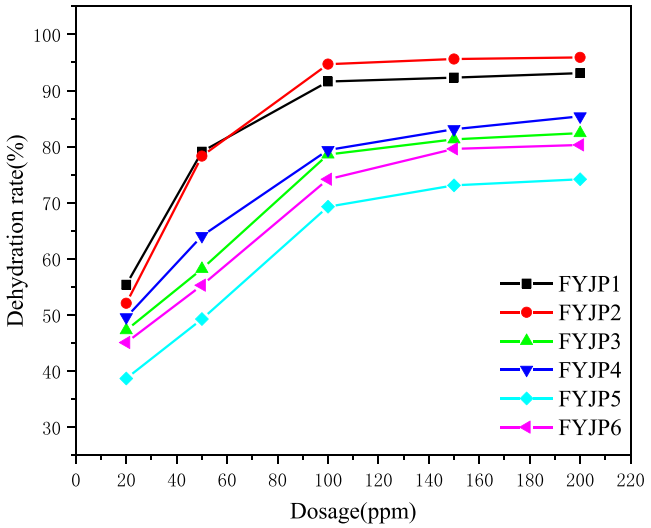

Figure 3. Effect of dosage on FYJP demulsification performance.

FYJP1 at various concentrations are higher than those of other FYJP demulsifiers. When the amount of the demulsifier is low (less than 20 ppm), the dehydration rate is also low. When the amount of the FYJP demulsifier is increased (20−100 ppm), the dehydration rate increases rapidly. Finally, when the dosage of the FYJP demulsifier is greater than 100 ppm, although the dehydration rate is still increasing, it is extremely slow and even tends to balance. This is because the higher the amount or concentration of the polyether demulsifier, the lower the interfacial tension at the oil−water interface, the lower the strength of the interfacial film at the oil−water interface, and the easier the demulsification and dehydration.[52] When the amount or concentration of the polyether demulsifier increases, the interfacial tension of oil and water decreases slowly, and the increase in the dehydration rate also slows down.[53,54] Although a high dosage or a high concentration of the FYJP demulsifier has a high dehydration rate, the cost of demulsification also increases due to the large increase in dosage of the demulsifier. To sum up, the optimal dosage of the FYJP polyether demulsifier is 100 ppm.

Demulsification Test. The moisture content of a crude oil emulsion measured by the distillation method is 23%. The demulsifier dosage of 100 ppm and the demulsifier temperature of 85 °C were set to conduct demulsification and dehydration tests on the synthesized YJP series and FYJP series demulsifiers. The amount of water removed from the tube during different time periods and the calculated dehydration rate were recorded. The experimental results are shown in Figures 4 and 5.

Figure 4a shows the dehydration rate of FYJP demulsifiers in different time periods, and Figure 4b intuitively reflects the amount of dehydration in each time period. The dehydration rate of FYJP demulsifiers increased the fastest in the first 60 min, and all of the other dehydration rates except that of FYJP5 were more than 65%. Moreover, according to Figure 4b, it can be seen that the amount of dehydration was most in the first 30 min, among which the dehydration rate of FYJP2 in 30 min was more than 40%, and its dehydration rate in 60 min was more than 80%. However, FYJP5 had the lowest dehydration rate, which was only 57% at 60 min. In two time periods of 60−90 min and 90−120 min, the amount of dehydration decreased, and the increase in the dehydration rate of the FYJP series demulsifiers decreased. The overall demulsification rate of the final modified FYJP polyether demulsifier was above 70%, and the dehydration rate of FYJP2 was the highest, reaching 94.7%.

Figure 4c shows the demulsification results of a W/O crude oil emulsion in Liaohe Oilfield by FYJP demulsifiers. It can be seen that the amount of dehydration of FYJP2 is significantly higher than that of the others by comparing the six test tubes. The demulsification and dehydration capacity was in the order FYJP2 > FYJP1 > FYJP4 > FYJP3 > FYJP6 > FYJP5. By comparing FYJP1, FYJP2, FYJP3, and FYJP4 in Figure 4a,c, it can be seen that when the PO content is constant, the amount of dehydration and the dehydration rate increase significantly as the EO content increases. This is because the hydrophilicity of the polyether demulsifier increases with the increase in the proportion of EO.[55,56] The improvement of hydrophilicity makes the demulsifier reach the oil−water surface faster, the surface tension of the oil−water interface is weakened, the strength of the interface membrane of the oil−water interface is reduced, and the dehydration rate is increased. But greater hydrophilicity is not always better. When the hydrophilic energy is too large, the amount of the demulsifier dissolved in water increases, which reduces the amount of the demulsifier adsorbed on the oil−water interface, resulting in a lower dehydration rate. Only when the hydrophilicity is a certain value do the dehydration rate and the demulsification rate reach the highest values.

As can be seen from Figure 5, the overall demulsification rate of an unmodified YJP polyether demulsifier is less than 70%, and YJP2 has the highest dehydration rate, which is only 68%. As can be seen from the comparison between Figures 4a and 5, the overall demulsification rate of the modified FYJP polyether demulsifier is more than 70%, with the highest reaching 94.7%. However, the overall demulsification rate of the unmodified YJP polyether demulsifier is less than 70%, and the overall demulsification rate of the FYJP polyether demulsifier is much higher than that of the YJP polyether demulsifier. This indicates that the demulsification performance of the modified demulsifier is better than that of the unmodified polyether demulsifier. At the same time, in terms of modified or unmodified polyether demulsifiers, the demulsification capacity of demulsifier no. 2 is higher than other types.

Microscopic Demulsification Process. The microscopic demulsification process of a W/O emulsion can be clearly observed in Figure 6. The dehydration ability of the FYJP demulsifier is excellent. The emulsion was very stable and the small water droplets were enveloped in the oil phase. At 30 min, demulsifier molecules began to adsorb on the oil−water interface film. The hydrophilic group extended to the water phase to attract small water droplets around. The hydrophobic group extended to the oil phase to replace natural emulsifiers such as asphaltene and reduced the thickness of the interface film. At 60 min, demulsifier molecules stretched on the oil−water interface and small water droplets combined to form large water droplets, which began to settle at the bottom of the test tube. At 90 min, the separation of oil and water in the W/O emulsion was stable and the number of water droplets decreased. At 120 min, the dehydration was completed, only small-diameter water droplets were left free in the emulsion, and almost no large water droplets were left.

Demulsification Mechanism. When the demulsifier is dispersed into the emulsion, due to its high surface activity and

https://doi.org/10.1021/acsomega.1c02352
ACS Omega 2021, 6, 17709−17719

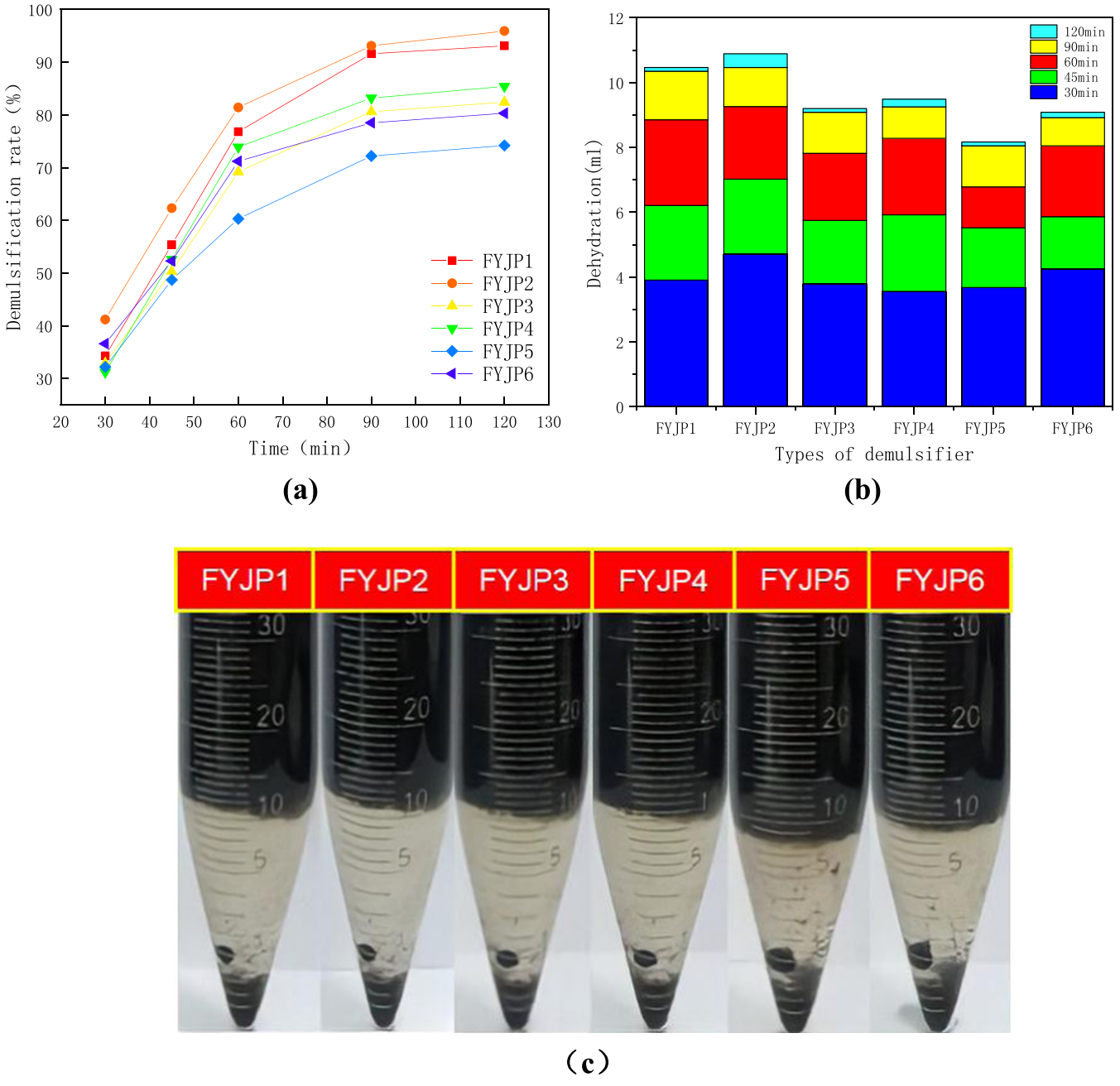

Figure 4. (a) Dehydration rate of FYJP demulsifiers in different time periods, (b) dehydration of FYJP series demulsifiers in different time periods, and (c) dehydration results of FYJP series demulsifiers at 120 min.

hydrophilic and oleophilic properties, it passes through the external phase of the emulsion to reach the oil–water interface and is adsorbed. The hydrophilic end of the demulsifier is adsorbed in the water layer, and the oil–water end is inserted into the oil layer. A large amount of the demulsifier is adsorbed on the oil–water surface at the same time to form a new layer of an oil–water interface membrane. The phenomenon of displacing or replacing the old interfacial membrane occurs. At the same time, in the state of external action, such as stirring, heating, etc., the new interfacial membrane ruptures due to its less stable nature. As a result, water droplets in the inner phase enter the outer phase and coalesce with other water droplets. When the droplets coalesce to a certain extent, they settle slowly under the action of gravity and form a water layer at the bottom to realize oil–water separation. With the decrease of water droplets in the emulsion, the coalescence probability of the remaining water droplets decreases, and the sedimentation rate of the bottom water phase slows down until the equilibrium demulsification is achieved. Figure 7 shows the demulsification mechanism diagram.

CONCLUSIONS

The preparation of an efficient demulsifier is essential for the demulsification and dehydration of an emulsion. In this paper, a new nonanionic polyether demulsifier was successfully synthesized and characterized. The measurement of the surface tension showed that the demulsifier features high surface activity and can effectively reduce the surface tension. The analyses of the cloud point, HLB values, and RSN values showed that the overall dehydration rate and demulsification

https://doi.org/10.1021/acsomega.1c02352
ACS Omega 2021, 6, 17709–17719

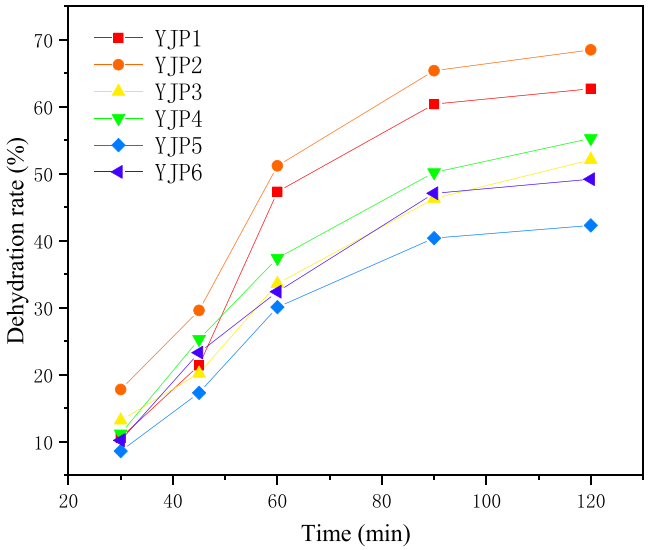

Figure 5. Dehydration rate of YJP demulsifiers in different time periods.

efficiency of the demulsifier increased as the hydrophilicity increased but did not exceed a certain value. The microscopic demulsification process of the demulsifier was studied, and it was proved that the FYJP demulsifier had fast diffusion and adsorption at the oil−water interface and excellent demulsification ability. The demulsification test illustrated that the demulsification performance of the modified demulsifier was much higher than that of the unmodified demulsifier. Alongside that, the optimal dosage of 100 ppm was determined by comparing and analyzing the dosage of different demulsifiers. The best demulsifier, FYJP2, was selected by a demulsification and dehydration test. The highest dehydration rate of the demulsifier was 94.7% at 85 °C, 100 ppm demulsifier dosage, and 120 min demulsification time.

EXPERIMENTAL SECTION

Materials. EO and PO were provided by the laboratory, methanol, *p-tert*-butylphenol (PTBP), potassium hydroxide, and formaldehyde (40 wt %) were purchased from Tianjin Tianli Chemical Reagent Co., Ltd, and triethylenetetramine was purchased from Tianjin Cameo Chemical Reagent Co., Ltd. In addition, sodium chloroacetate was provided by the Tianjin Damao Chemical Reagent Factory. All of the abovementioned drugs and reagents were of analytically pure grade. The physicochemical properties of the crude oil taken from Liaohe Oilfield are shown in Table 2.

Synthesis of Nonionic Polyether Demulsifiers. To begin with, 30 g of *p-tert*-butylphenol (PTBP) and 58.4 g of triethylenetetramine were put into a three-neck flask, which was placed in an oil bath and heated to 50 °C. After 15 min of heat preservation, 30 g (40 wt %) of formaldehyde solution was slowly added into three three-mouth flask using a separating funnel. After dripping, the solution was kept warm for 30 min. Then, 60 g of methanol was poured into the flask on which the condensing reflux device was installed, and the oil bath temperature was increased to 110 °C for reflux dehydration for 2 h. After that, the temperature was increased to 150 °C again to steam out the methanol. During the process of a 1 h reaction, the material transparency in the flask needed to be observed. The final step was to cool the flask and pour out the internal solution to get the initiator.

A total of 5 g of the initiator obtained from the above reaction and 0.70 g of potassium hydroxide were added to the reactor with high temperature and high pressure. N_2 was employed to replace the air in the reactor. The gas in the high-pressure reactor was pumped out by a vacuum pump, and the pressure indicator was observed to stop when it reached negative pressure. Overall, 345 g of epoxy propane (PO) was slowly fed into the feed port and heated to 130 °C, and the pressure gauge reading was maintained at about 0.2 MPa. The feed valve was closed when the feed was completely finished. The first step of the reaction ended when the pressure indicator was reduced to negative pressure.

Following the first step of the experiment, 0.71 g of potassium hydroxide was put in the high-pressure reactor again, and 127.8 g of ethylene oxide (EO) was passed into the reactor in the same way for the polymerization reaction, and finally the nonionic polyether demulsifier YJP1 was obtained by cooling and opening the reactor; the mass ratio of its initiator to propylene oxide (PO) was 1:69, and the mass ratio of propylene oxide (PO) to ethylene oxide (EO) was 2.7:1.

In each experiment, the mass ratios of the initiator to propylene oxide (PO) were 1:69, 1:99, and 1:159. The mass

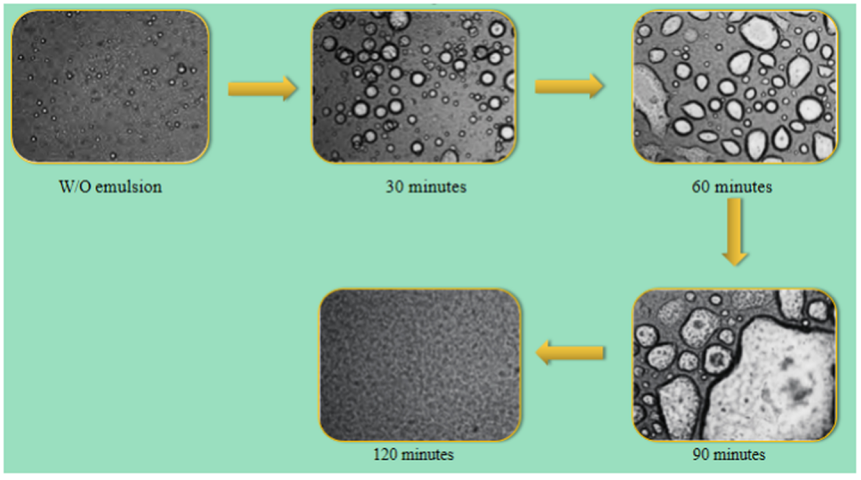

Figure 6. Microscopic demulsification process.

https://doi.org/10.1021/acsomega.1c02352
ACS Omega 2021, 6, 17709−17719

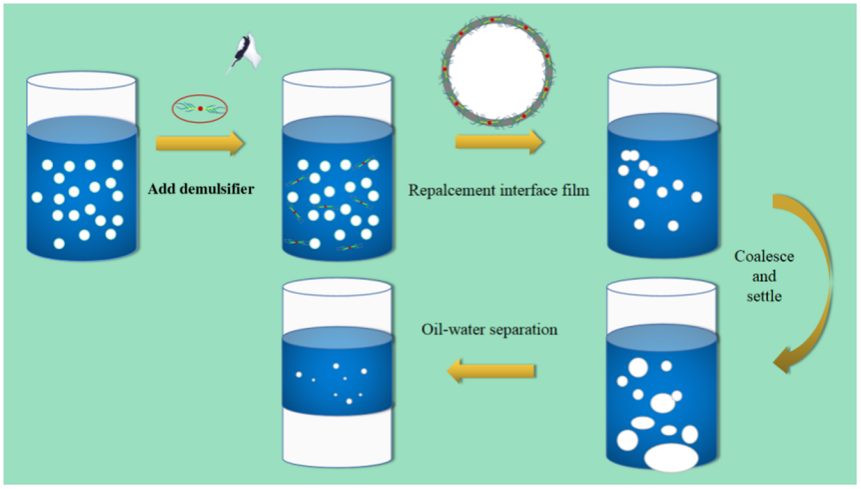

Figure 7. Demulsification mechanism diagram.

Table 2. Basic Physical Properties of Crude Oil Produced in a Block of Liaohe Oilfield

density (kg·m^{-3})	dynamic viscosity (50 °C) (mPa·s)	gum (%)	asphaltene (%)	acid value (mgKOH·g^{-1})	pour point (°C)	sulfur content (%)
920.6	219.1	14.34	8.47	1.93	16	0.158

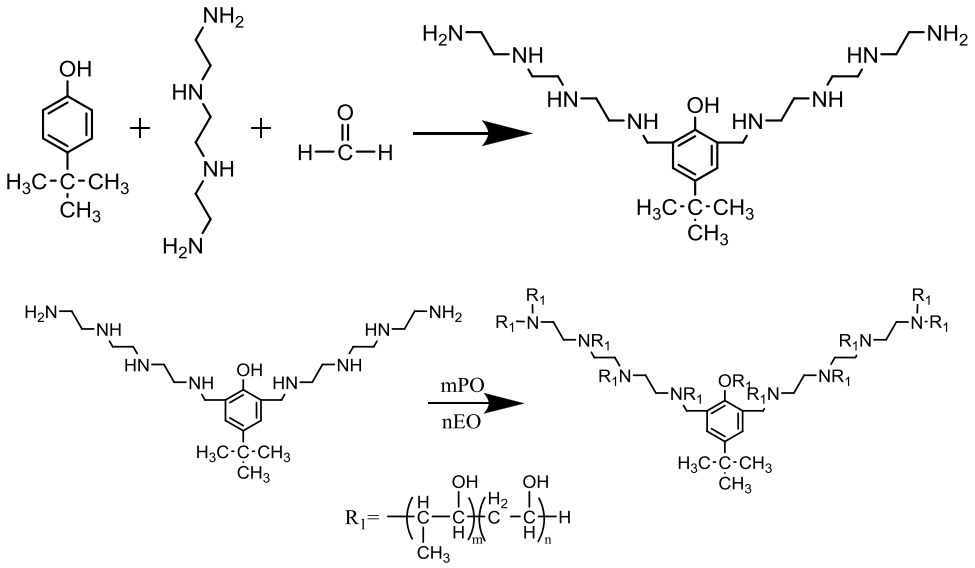

Figure 8. Polymerization formula of demulsifiers.

ratios of propylene oxide (PO) and ethylene oxide (EO) were 2.7:1 and 3.7:1.

Figure 8 shows the specific polymerization formula of demulsifiers, and Table 3 shows the synthesis ratio of the YJP demulsifiers.

Modification of the Nonionic Polyether Demulsifiers. A total of 20 g of a nonionic polyether demulsifier was added to a three-neck flask, which was placed in an oil bath, stirred, and heated to 50 °C. Next, 0.6 g (40 wt %) of potassium hydroxide solution was added with a gel head dropper and stirred for 20 min at 150 rpm. The temperature was increased again to 65 °C, and 1.3 g (30 wt %) of sodium chloroacetic acid solution was slowly added with a separating funnel, and the drip was finished at about 2.5 h with a controlled drip acceleration. After dripping, the temperature was increased to 85 °C, and the reaction ended after 8 h of heat preservation. After cooling, water and methanol were added to prepare 50 wt % of the sample to obtain the FYJP nonanionic polyether demulsifier. In the configuration of 30 wt % sodium chloroacetate solution, the mass ratio of sodium chloroacetate, methanol, and water was 10:16.3:7.

Figure 9 shows the modification reaction equation of the nonionic polyether demulsifier. Figure 10 shows a schematic diagram of the chemical synthesis of the FYJP nonanionic polyether demulsifier.

Table 3. Synthesis Ratio of the YJP Demulsifiers

demulsifier sample	initiator/PO	PO/EO	demulsifier sample	initiator/PO	PO/EO
YJP1	1:69	3.7:1	YJP4	1:99	2.7:1
YJP2	1:69	2.7:1	YJP5	1:159	3.7:1
YJP3	1:99	3.7:1	YJP6	1:159	2.7:1

https://doi.org/10.1021/acsomega.1c02352
ACS Omega 2021, 6, 17709−17719

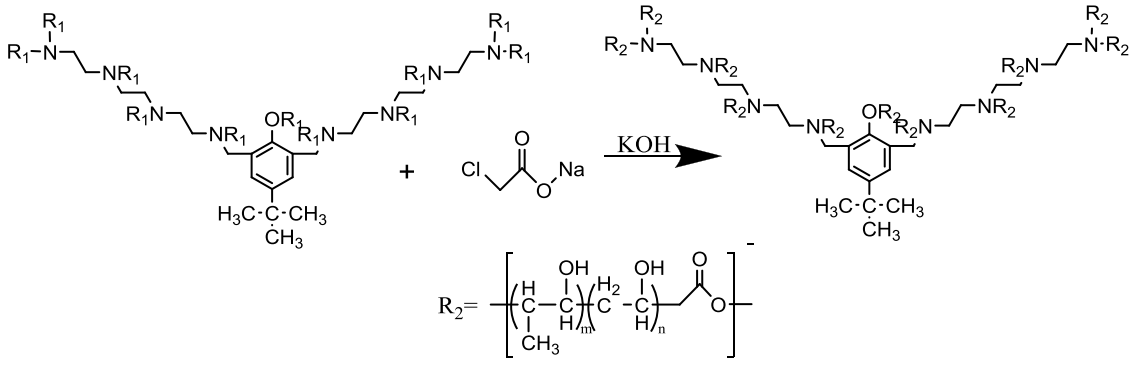

Figure 9. Modification equation of the polyether demulsifier.

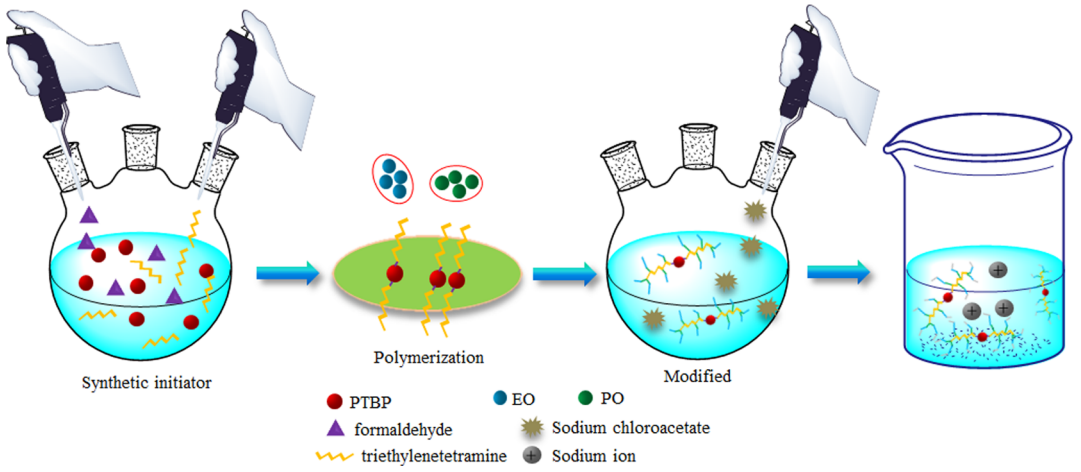

Figure 10. Schematic diagram of chemical synthesis of modified polyether demulsifiers.

Determination of the Cloud Point and the HLB Value of the Demulsifiers. The turbidity point method is used to measure the turbidity point of nonanion polyether demulsifiers. The FYJP synthetic nonanionic polyether demulsifier was configured as a 10 wt % aqueous solution in a test tube; the thermometer was mounted on the test tube, and the height of the liquid level was controlled at 70 mm. The tubes were heated in an oil bath, controlled for a gradual increase in temperature, and the solution was observed. When the solution appeared cloudy, the value on the thermometer needed to be read quickly. After cooling the tube to room temperature, the abovementioned experimental steps were repeated and the data were obtained. All of the data were collated and averaged to obtain the cloud point of the demulsifier.

The hydrophilic−lipophilic balance (HLB) value of polyether demulsifiers has a certain quantitative relationship with the cloud point. The HLB value can be calculated from the cloud points obtained in the abovementioned experiments, and the calculation formula is shown as eq 1.[57]

$$\mathrm{HLB} = 0.0980X + 4.02 \quad (1)$$

X is the cloud point value of the 10 wt % FYJP polyether demulsifier.

Determination of Relative Solubility (RSN) of Demulsifiers. A total of 30 mL of the prepared titration solution (mixed with 2.6 vol % toluene and 97.4 vol % ethylene glycol dimethyl ether) was poured into a beaker, and 1 g of the polyether demulsifier was dropped, stirred with a glass rod until the mixture was uniform, titrated with distilled water until the solution became turbid for 1 min or longer, and the volume of titrated distilled water was recorded, which was the RSN value of the demulsifier.

Determination of Interfacial Tension of Demulsifiers. A Kruss DSA100 contact angle measuring instrument was used for measuring modified polyether demulsifiers. The polyether aqueous solutions with different concentrations were heated in a water bath after being prepared and then measured at a set temperature of 80 °C. A 1 mL disposable syringe was selected as the instrument of the hanging drop method to measure the interfacial tension of polyether aqueous solutions with different concentrations.

Experiment on Demulsification and Dehydration of the Demulsifiers. Preparation experiment of the W/O crude oil emulsion: A certain amount of crude oil and sewage was weighed and preheated at 65 °C for 1 h. The mixer was started and sewage was gradually added into the crude oil at a stirring speed of 7000 rpm. After adding water and stirring for 15 min, a stable W/O crude oil emulsion was obtained.

Determination of the moisture content of the W/O type crude oil emulsion by distillation: The emulsion was heated to flow at 65 °C and poured into a round-bottom flask containing diesel oil with a few shards of porcelain at the bottom to prevent the liquid from boiling over. The condensing tube and the receiver were installed, the distillation flask was heated in a constant temperature oil bath, and the drop rate of the condensate was controlled to approximately 4 drops/s until there was no more water in the distillation unit and the volume of the liquid in the receiver had not changed for a period of time. Next, heating was stopped and then the mixture was

https://doi.org/10.1021/acsomega.1c02352
ACS Omega 2021, 6, 17709−17719

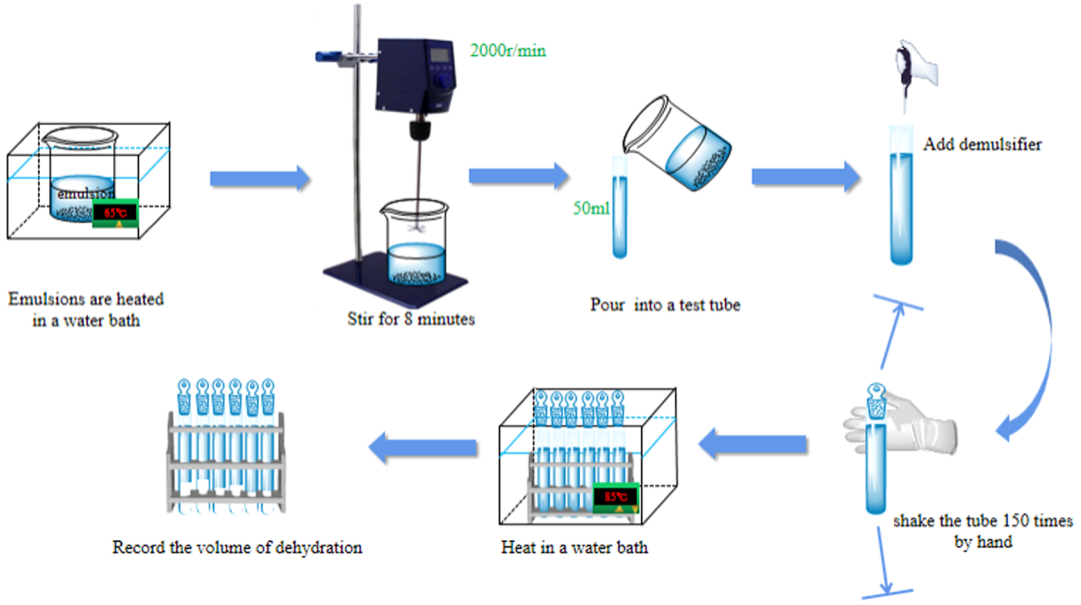

Figure 11. Schematic diagram of the demulsification and dehydration experiment.

cooled to room temperature. The water droplets attached to the receiver were scraped into the liquid with a tool, and the volume of water in the receiver was read. The volume fraction of water in the crude oil emulsion was calculated according to formula 2.[58]

$$\varphi = \frac{(V_1 - V_0)}{V} \times 100\% \quad (2)$$

φ is the volume fraction of water, V_1 is the volume of separated water of the blank experimental control, V_0 is the volume of separated water in the receiver, and V is the volume of the crude oil emulsion.

The demulsification temperature was selected as 85 °C, which was consistent with the actual demulsification temperature in the oil plant. The emulsion was heated in a water bath until it began to flow, and the upper emulsion was placed in a beaker and put into an electric stirrer at a speed of 2000 rpm for 8 min and then put aside for 5 min; then, 50 mL was poured into a tapered graduated tube. A small amount of the FYJP nonanionic polyether demulsifier was added to the test tube; the test tube was shaken by hand 150 times and heated in a water bath at the temperature specified above. Each tapered scale tube retained a set of blank controls to record the volume of water released at different times. The demulsification efficiency can be calculated by the volume of demulsified water and the volume of water in the emulsion, as shown in eq 3.[41]

$$W\ (\%) = \frac{V_w}{V_r} \times 100 \quad (3)$$

W is the demulsification rate of the demulsifier for the heavy oil emulsion, V_r is the volume of water from the emulsion, and V_w is the volume of emulsion dehydration under the action of the demulsifier.

Figure 11 shows a schematic diagram of the demulsification and dehydration experiment.

Microscopic Demulsification Process Test. A W/O emulsion with 0.1 g L^{-1} FYJP demulsifier was evenly spread on the glass slides at 25 °C. A BH-2 microscope was used for observation. Microdemulsifier processes at different time periods were recorded using SPECTRUMSEE-ADVANCE software.

AUTHOR INFORMATION

Corresponding Authors

Lin Zhang − *School of Petroleum Engineering, Northeast Petroleum University, Daqing 163318, China;* orcid.org/0000-0002-9740-1980; Email: 948689953@qq.com

Xinlei Jia − *College of Chemical Engineering ashaind Safety, Binzhou University, Binzhou 256600, China;* Email: 1004024260@qq.com

Authors

Lixin Wei − *School of Petroleum Engineering, Northeast Petroleum University, Daqing 163318, China*

Meng Chao − *Gas Production Branch of Daqing Oilfield Co Ltd., Daqing 163453, China*

Chao Liu − *School of Petroleum Engineering, Northeast Petroleum University, Daqing 163318, China*

Lijun Shi − *School of Petroleum Engineering, Northeast Petroleum University, Daqing 163318, China*

Complete contact information is available at: https://pubs.acs.org/10.1021/acsomega.1c02352

Notes

The authors declare no competing financial interest.

ACKNOWLEDGMENTS

The authors are grateful for the reviewers' instructive suggestions and careful proofreading. This work was supported by the Natural Science Foundation of Shandong Province for Youth (grant no. ZR2020QE111), the Doctoral Research Startup Project of Binzhou University (grant no. 2019Y27), and the Postdoctoral Science Foundation of China (grant no. 2020M681073).

REFERENCES

(1) Flaaten, A. K.; Nguyen, Q. P.; Zhang, J.; Mohammadi, H.; Pope, G. A. Alkaline/surfactant/polymer chemical flooding without the need for soft water. *SPE. J.* **2010**, *15*, 184−196.

(2) Park, S.; Lee, E. S.; Sulaiman, W. Adsorption behaviors of surfactants for chemical flooding in enhanced oil recovery. *J. Ind. Eng. Chem.* **2015**, *21*, 1239−1245.
(3) Kamari, A.; Sattari, M.; Mohammadi, A. H.; Ramjugernath, D. Reliable method for the determination of surfactant retention in porous media during chemical flooding oil recovery. *Fuel* **2015**, *158*, 122−128.
(4) Arjmand, O.; Kalbasi, M.; Roostaei, A. R. Experimental study of chemical flooding using new chemical component to enhance oil recovery. *Res. J. Appl. Sci., Eng. Technol.* **2012**, *4*, 3056−3061.
(5) Sun, L.; Xiaolin, W. U.; Zhou, W.; Xuejun, L. I.; Han, P. Technologies of enhancing oil recovery by chemical flooding in daqing oilfield, ne china. *Pet. Explor. Dev.* **2018**, *45*, 673−684.
(6) Feitosa, F. X.; Alves, R. S.; Sant'Ana, H. D. Synthesis and application of additives based on cardanol as demulsifier for water-in-oil emulsions. *Fuel* **2019**, *245*, 21−28.
(7) Pereira, J. C.; Delgado-Linares, J.; Scorzza, C.; Rondo, N. M.; Rodri Guez, S.; Salager, J. L. Breaking of water-in-crude oil emulsions. 4. estimation of the demulsifier surfactant performance to destabilize the asphaltenes effect. *Energy Fuels* **2011**, *25*, 1045−1050.
(8) Soema, P. C.; Kompier, R.; Amorij, J.-P.; Kersten, G. F. A. Current and next generation influenza vaccines: formulation and production strategies. *Eur. J. Pharm. Biopharm.* **2015**, *94*, 251−263.
(9) Yang, J.; Ban, W.; Han, Z.; Xu, X. Demulsification of produced liquid from surfactant-polymer flooding. *J. Dispersion Sci. Technol.* **2019**, *40*, 487−494.
(10) Wu, M.; Zhai, M.; Li, X. Adsorptive removal of oil drops from asp flooding-produced water by polyether polysiloxane-grafted zif-8. *Powder Technol.* **2021**, *378*, 76−84.
(11) Walstra, P. Principles of emulsion formation. *Chem. Eng. Sci.* **1993**, *48*, 333−349.
(12) Guttoff, M.; Saberi, A. H.; Mcclements, D. J. Formation of vitamin d nanoemulsion-based delivery systems by spontaneous emulsification: factors affecting particle size and stability. *Food Chem.* **2015**, *171*, 117−122.
(13) Detrembleur, C.; Debuigne, A.; Bryaskova, R.; Charleux, B.; Robert, J. Cobalt-mediated radical polymerization of vinyl acetate in miniemulsion: very fast formation of stable poly (vinyl acetate) latexes at low temperature. *Macromol. Rapid Commun.* **2006**, *27*, 37−41.
(14) Ma, L.; Chen, Y.; Liu, Y.; Chen, M.; Zhang, B.; Yue, D. Investigation the performance of a block polyether demulsifier based on polysiloxane for the treatment of aged oil. *Energy Fuels* **2017**, *9*, 8886−8895.
(15) Yang, Y.; Feng, J.; Cao, X. L.; et al. Effect of Demulsifier Structures on the Interfacial Dilational Properties of Oil−Water Films. *J. Dispersion Sci. Technol.* **2016**, *37*, 1050−1058.
(16) Sun, H.; et al. Novel polyether-polyquaternium copolymer as an effective reverse demulsifier for O/W emulsions: Demulsification performance and mechanism. *Fuel* **2020**, *263*, No. 116770.
(17) Ma, B.; Zhu, J. Evaluation of demulsifiers for demulsification/dehydration of venezuela heavy crude oil and optimizing electrical desalting operation conditions. *Pet. Process. Petrochem.* **2012**, *43*, 98−102.
(18) Li, S.; Li, N.; Yang, S.; Liu, F.; Zhou, J. The synthesis of a novel magnetic demulsifier and its application for the demulsification of oil-charged industrial wastewaters. *J. Mater. Chem. A* **2014**, *2*, 94−99.
(19) Kanazawa, S.; Takahashi, Y.; Nomoto, Y. Emulsification and demulsification processes in liquid−liquid system by electrostatic atomization technique. *IEEE Trans. Ind. Appl.* **2008**, *44*, 1084−1089.
(20) Akay, G.; Pekdemir, T.; Shakorfow, A. M.; Vickers, J. Intensified demulsification and separation of thermal oxide reprocessing interfacial crud (thorp-ifc) simulants. *Green Process. Synth.* **2012**, *1*, 109−127.
(21) Nikkhah, M.; Tohidian, T.; Rahimpour, M. R.; Jahanmiri, A. Efficient demulsification of water-in-oil emulsion by a novel nano-titania modified chemical demulsifier. *Chem. Eng. Res. Des.* **2015**, *94*, 164−172.
(22) Alves, R. S.; Maia, D. L. H.; Fernandes, F. A. N.; Feitosa, F. X.; de Sant'Ana, H. B. Synthesis and application of castor oil maleate and castor oil maleate-styrene copolymers as demulsifier for water-in-oil emulsions. *Fuel* **2020**, *269*, No. 117429.
(23) Chen, Y.; Tian, G.; Liang, H.; Liang, Y. Synthesis of magnetically responsive hyperbranched polyamidoamine based on the graphene oxide: Application as demulsifier for oil ater emulsions. *Int. J. Energy Res.* **2019**, *43*, 4756−4765.
(24) Beetge, J. H.; Horne, B. Chemical-demulsifier development based on critical-electric-field measurements. *SPE J.* **2008**, *13*, 346−353.
(25) Yao, X.; Jiang, B.; Zhang, L.; Sun, Y.; Xiao, X.; Zhang, Z.; Zhao, Z. Synthesis of a novel dendrimer-based demulsifier and its application in the treatment of typical diesel-in-water emulsions with ultrafine oil droplets. *Energy Fuels* **2014**, *28*, 5998−6005.
(26) Buddin, M. M. H. S.; Ahmad, A. L.; Khalil, A.; Puasa, S. W. A review of demulsification technique and mechanism for emulsion liquid membrane applications. *J. Dispersion Sci. Technol.* **2020**, 1−18.
(27) Li, X.; Kersten, S.; Schuur, B. Efficiency and mechanism of demulsification of oil-in-water emulsions using ionic liquids. *Energy Fuels* **2016**, *30*, 7622−7628.
(28) Bello, A.; Umar, A. A. Effect of native solids sizes and concentrations on the kinetic stability of water-in-oil emulsions. *IOP Conf. Ser.: Mater. Sci. Eng.* **2020**, *884*, No. 012028.
(29) Smits, J.; Giri, R. P.; Chen, S.; Mendona, D.; Maas, M.; et al. Synergistic and competitive adsorption of hydrophilic nanoparticles and oil-soluble surfactants at the oil-water interface. *Langmuir* **2021**, 5659−5672.
(30) Souza, A. V.; Mendes, M.; Souza, S.; Palermo, L.; Pf, O. E.; Mansur, C. Synthesis of additives based on polyethylenimine modified with non-ionic surfactants for application in phase separation of water-in-oil emulsions. *Energy Fuels* **2017**, *31*, 10612−10619.
(31) Kailey, I.; Blackwell, C.; Behles, J. Effects of crosslinking in demulsifiers on their performance. *Can. J. Chem. Eng.* **2013**, *91*, 1433−1438.
(32) Nguyen, D.; Sadeghi, N.; Houston, C. Chemical interactions and demulsifier characteristics for enhanced oil recovery applications. *Energy Fuels* **2012**, *26*, 2742−2750.
(33) Niu, Z.; Yue, T.; He, X.; Manica, R. Changing the interface between an asphaltene model compound and water by addition of an eo-po demulsifier through adsorption competition or adsorption replacement. *Energy Fuels* **2019**, *33*, 5035−5042.
(34) Kaniwa, M.; Ikarashi, Y.; Kojima, S.; Nakamura, A.; Shono, M.; Ezoe, K. Chemical approach to contact dermatitis caused by household products. vii. p-tert-butylphenol formaldehyde resin in commercially available adhesive tapes, shoes and adhesives for rubber and leather. *Eisei Kagaku* **1991**, *37*, 58−67.
(35) Lu, Y.; Chen, X. The effects of a demulsifier on the interface of marine engine oil and water. *Lubr. Sci.* **2011**, *23*, 293−298.
(36) Li, Z.; Geng, H.; Wang, X.; Jing, B.; Liu, Y.; Tan, Y. Noval tannic acid-based polyether as an effective demulsifier for water-in-aging crude oil emulsions. *Chem. Eng. J.* **2018**, *354*, 1110−1119.
(37) Klaus, A.; Tiddy, G.; Rachel, R.; Trinh, A. P.; Maurer, E.; Touraud, D.; Kunz, W. Hydrotrope-induced inversion of salt effects on the cloud point of an extended surfactant. *Langmuir* **2011**, *27*, 4403−4411.
(38) Lv, W.; Gong, H.; Li, Y.; Qian, S.; Xu, L.; Dong, M. Dissolution behaviors of alkyl block polyethers in co2: experimental measurements and molecular dynamics simulations. *Chem. Eng. Sci.* **2020**, *228*, No. 115953.
(39) Wei, L.; Chao, M.; Dai, X.; Jia, X.; Geng, X.; Guo, H. (2021). Synthesis and characterization of a novel multibranched block polyether demulsifier by polymerization. *ACS Omega* **2021**, *6*, 10454−10461.
(40) Jia, H.; Lian, P.; Liang, Y.; Zhu, Y.; Huang, P.; Wu, H.; Leng, X.; Zhou, H. Systematic investigation of the effects of zwitterionic surface-active ionic liquids on the interfacial tension of a water/crude oil system and their application to enhance crude oil recovery. *Energy Fuels* **2018**, *32*, 154−160.

https://doi.org/10.1021/acsomega.1c02352
ACS Omega 2021, 6, 17709−17719

(41) Kailey, I. Key performance indicators reveal the impact of demulsifier characteristics on oil sands froth treatment. *Energy Fuels* **2017**, *31*, 2636−2642.
(42) Pradilla, D.; Ramírez, J.; Zanetti, F.; Álvarez, O. Demulsifier performance and dehydration mechanisms in colombian heavy crude oil emulsions. *Energy Fuels* **2017**, *31*, 10369−10377.
(43) Krstonoi, V. S.; Kali, M. D.; Dapevi-Hadnaev, T. R.; Lonarevi, I. S.; Hadnaev, M. S. Physico-chemical characterization of protein stabilized oil-in-water emulsions. *Colloids Surf., A.* **2020**, *602*, No. 125045.
(44) Liu, Y.; et al. Surface tension of supercooled graphene oxide nanofluids measured with acoustic levitation. *J. Therm. Anal. Calorim.* **2020**, *144*, 1369−1379.
(45) Bergström, L. M.; Tehrani-Bagha, A.; Nagy, G. Growth behavior, geometrical shape, and second cmc of micelles formed by cationic gemini esterquat surfactants. *Langmuir* **2015**, *31*, 4644−4653.
(46) Buddin, M.; Ahmad, A.; Khalil, A.; Puasa, S. Self-assembly and rheological behavior of chloramphenicol-based poly(ester ether)-urethanes. *J. Polym. Res.* **2021**, *28*, 1−15.
(47) Shi, Y.; Hong, Q. L.; Li, N. B. Determination of the critical premicelle concentration, first critical micelle concentration and second critical micelle concentration of surfactants by resonance rayleigh scattering method without any probe. *Spectrochim. Acta, Part A* **2011**, *78*, 1403−1407.
(48) Rikiyama, K.; Horiuchi, T.; Koga, N.; et al. Mceclizaion of poly(ethylene oxide)-poly(propylene oxide) alternating multiblock copolymers in water. *Polymer* **2018**, *156*, 102−110.
(49) Danov, K. D.; Kralchevsky, P. A.; Stoyanov, S. D.; et al. Analyticalmodeling of micelle growth.2. Molecular thermodynamics of mixed aggregatesand sission energy in wormlike micelles. *J. Colloid Interface Sci.* **2019**, *551*, 227−241.
(50) Naqvi, A. Z.; Kabir, U. D. Clouding phenomenon in amphiphilic systems: Areview of five decades. *Colloids Surf., B* **2018**, *165*, 325−344.
(51) Kailey, I. Key Perfomnance Indicators Reveal the Impact of Demulsifer Characterstics on Oil Sands Froth Treatment. *Energy Fuels* **2017**, *31*, 2636−2642.
(52) Feng, X.; Mussone, P.; Gao, S.; Wang, S.; Wu, S. Y.; Masliyah, J. H.; Xu, Z. Mechanisticstudy on demulsification of water-in-diluted bitumen emulsions by ethylcellulose. *Langmuir* **2010**, *26*, 3050−3057.
(53) Pensini, E.; Harbottle, D.; Yang, F.; Tchoukov, P.; Li, Z.; Kailey, I.; Behles, J.; Masliyah, J.; Xu, Z. Demulsification mechanism of asphaltene-stabilized water-in-oil emulsionsby a polymeric ethylene oxide-propylene oxide demulsifier. *Energy Fuels* **2014**, *28*, 6760−6771.
(54) Feng, X.; Xu, Z.; Masliyah, J. Biodegradable polymer for demulsification of water-inbitumen emulsions. *Energy Fuels* **2009**, *23*, 451−456.
(55) Maccarrone, S.; Allgaier, J.; Frielinghaus, H.; Richter, D. Anchoring vs bridging: new findings on polymer additives in bicontinuous microemulsions. *Langmuir* **2014**, *30*, 1500−1505.
(56) Li, Z.; Shi, Z.; Zhao, S.; Yin, S.; Tan, G.; Jing, B.; Tan, Y. Synthesis and properties of a novel branched polyether surfactant. *J. Surfactants Deterg.* **2016**, *19*, 1107−1120.
(57) Wang, J.; Li, C. Q.; An, N.; Yang, Y. Synthesis and demulsification of two lowergeneration hyperbranched polyether surfactants. *Sep. Sci. Technol.* **2012**, *47*, 1583−1589.
(58) Gotsche, M.; Wood, C.; Tiefensee, K. Preparation of W/O Emulsions. U.S. Patent US6,444,785B12002.

https://doi.org/10.1021/acsomega.1c02352
ACS Omega 2021, 6, 17709−17719